Volume 8, Issue 3, 2018, 3314 - 3318 ISSN 2069-5837

Biointerface Research in Applied Chemistry

www.BiointerfaceResearch.com

Original Research Article Open Access Journal

Received: 10.04.2018 / Revised: 20.05.2018 / Accepted: 25.05.2018 / Published on-line: 15.06.2018

Laser vaporization and controlled condensation (LVCC) of graphene supported Pd/Fe_3O_4 nanoparticles as an efficient magnetic catalysts for Suzuki Cross – Coupling

Hany A. Elazab [1, *]

[1]Department of Chemical Engineering, The British University in Egypt, Cairo, Egypt.

*corresponding author e-mail address:elazabha@vcu.edu

ABSTRACT

Herein, a reproducible, reliable, and efficient method was reported for the synthesis of palladium nanoparticles dispersed on a composite of Fe_3O_4 and graphene (Pd-Fe_3O_4/G) as a highly efficient active catalyst for being used in Suzuki cross–coupling reactions. Graphene supported Pd/Fe_3O_4 nanoparticles (Pd-Fe_3O_4/G) exhibit a remarkable catalytic performance towards Suzuki coupling reactions. Moreover, the prepared catalyst could be recycled for up to three times with high catalytic activity. The catalyst was prepared using LVCC synthesis; the prepared catalyst is highly magnetic which provides a platform to facilitate the separation process of the catalyst through applying an external magnetic field using a magnet. This adopted approach has several advantages including recyclability, mild reaction conditions, and reproducibility. The high catalytic activity is due to the catalyst-support strong interaction. Moreover, the defect sites found on reduced GO nanosheets act as nucleation centers providing a platform to anchor Pd and Fe_3O_4 nanoparticles and hence avoid the potential agglomeration and subsequently the anticipated decrease in the catalyst catalytic activity as a direct impact for this unfavorable agglomeration.

Keywords: *Graphene; Cross-Coupling; Magnetite (Fe_3O_4); LVCC synthesis; Catalyst recycling.*

1. INTRODUCTION

(This scientific research reports a reliable technique for synthesis of graphene supported nanoparticles using Laser Vaporization and Controlled Condensation (LVCC) for catalytic applications in the Suzuki cross-coupling reaction.[1-4] This method is generally one of the earliest methods for producing nanoparticles by preparing it directly from a supersaturated vapor.[5-13] There are some advantages of using this technique like high purity of produced nanoparticles, producing films and coatings, production of high density vapor of any metal within a short time (1014 atoms / 10 ns), directional high speed vapor, simultaneous or Sequential evaporation of several metal targets or alloys, formation of selected oxides, sub-oxides and non-stoichiometric oxides by controlling the partial pressure of oxygen, formation of nanoparticles of metals, oxides, alloys, filaments, carbides, sulfides, etc.[13-16]

There is also some disadvantages like the high cost per gram of material, difficulty to produce large quantities of materials. The LVCC method is based mainly on nanoparticles formation through condensation from the vapor phase. In LVCC method, the process consists of pulsed laser vaporization of a metal target into a selected gas mixture in a cloud chamber. The laser vaporization produces a high-density vapor a very short time - "10^{-8} s", in a directional jet that allows the directed deposition process.[5-7, 12, 17-19]

Until recently, two-dimensional materials were considered thermodynamically unstable and therefore could not exist. Then in 2004 the discovery of graphene quickly elevated it to a status of potential wonder material for a wide range of technological applications.[20] Graphene is a two-dimensional carbon allotrope containing a single atomic layer of sp^2 hybridized aromatic carbons appearing as a honeycomb type structure. The potential of graphene in the scientific community lies in its novel characteristics of being extremely thin, mechanically strong, transparent, as well as possessing high electrical and thermal conductivities.[21-23] These characteristics differ from other carbon allotropes because of graphene's two-dimensional structure where electron movement is limited to a narrower space opposed to a three-dimensional structure.[24-28]

There are a variety of methods for the preparation of graphene, among them is the reductions of graphene oxide (GO) using LVCC. This method provides a less toxic and shorter time of reaction than most conventional methods for the creation of graphene.

The potential of graphene as a support for Pd-catalysts in the Suzuki cross-coupling reaction can have many advantages. The Suzuki cross-coupling is a catalyzed reaction between aryl boronic acid and an aryl halide producing a biaryl compound. The benefits of graphene support are the provided thermal and chemical stability and reusability with limited loss in activity.[24-32] The catalytic activity is greatly influenced by the size distribution of the Pd/G, the smaller the size of each particle the larger the total surface area available becomes, increasing activity. After the exfoliation and reduction of GO, graphene is left with several defects scattered across its lattice which promote Pd-G interactions improving catalytic activity.[33-35] These defects along with carbon bonding provide an electron-rich support which stabilizes the metal nanoparticles preventing them from migrating and forming clusters that would decrease catalytic activity.[24-28] LVCC has the potential to create a smaller size distribution of the synthesized nanoparticles on graphene support, which ultimately would increase the effectiveness of this method for catalysis in the Suzuki cross-coupling reaction. LVCC utilizes a high powered

pulsed laser to ablate a bulk sample as well as control over the temperature gradient—providing convection, pressure, laser power and the atmosphere.[8-11, 13-16] The laser irradiates the target creating high density vapor while the inert atmosphere and convection current prevent the vaporized particles from growing into larger particles as they condense and deposit on the upper plate of the chamber.[5-7, 12, 17-19]

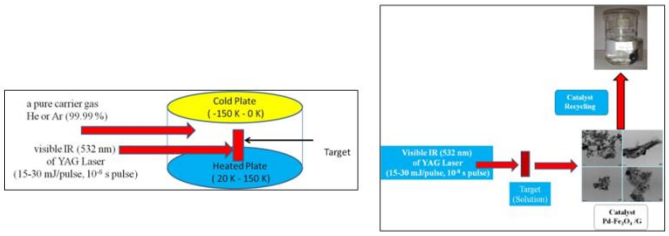

Figure 1. Experimental set-up for the synthesis of nanoparticles from (left) Solid (right) Solution using LVCC.

The previous sketch for the cloud chamber used in LVCC method shows that it consists of two horizontal, circular stainless steel plates, separated by a glass ring.

The metal target of interest "Pd for example" is fixed on the lower plate, and the chamber is filled with a pure carrier gas such as He or Ar (99.99 %) which are used because they are not reactive gases in case we don't need oxide formation which is happened in case of using a mixture containing a known composition of a reactant gas (e.g O_2 in case of oxides). It is important to maintain the metal target and the lower plate at a temperature higher than that of the upper one. The top plate can be cooled to less than 150 K by circulating liquid nitrogen (-150 – 0 K), and the lower plate (20-150 K). This large temperature gradient between the bottom and top plates results in a convection current which can be enhanced by using a heavy carrier gas like Ar under high pressure conditions of nearly 10^3 torr. Convection is important because it decreases the residence time by making circulation.[1-4]

So, Ar is better than He as a carrier gas because it is heavier than He, hence it convects more. The metal vapor is generated by pulsed laser vaporization using visible IR (532 nm) of YAG Laser (15-30 mJ/pulse, 10^{-8} s pulse). The laser beam is moved on the metal surface in order to expose new surface to the beam. The role of convection in the experiments is to remove the small particles away from the nucleation zone (once condensed out of the vapor phase) before they can grow into larger particles.[18, 36-40]

The rate of convection increases with the temperature gradient in the chamber. Therefore, by controlling the temperature gradient, the total pressure and the laser power. Generally this reaction utilizes pure Pd as the catalyst, which poses problems in recyclability and recovery. The substitution with a heterogeneous Pd catalyst could improve these difficulties but catalytic activity would be sacrificed. In an attempt to optimize recyclability, recovery and catalytic activity, the effects of varying compositions of Pd and Fe with graphene support were investigated with catalysis and characterized using UV-Visible Spectroscopy, Fourier Transform-Infrared (FT-IR) Spectroscopy, X-ray Photoelectron Spectroscopy (XPS) as well as tested for magnetic properties.

2. EXPERIMENTAL SECTION

Metal powders had been mixed according to calculations creating pellets with varying compositions of Fe/GO, Pd/GO and Pd-Fe/GO consisting of Fe/GO (20 wt% Fe - 80 wt% GO), Pd/GO (20 wt% Pd - 80 wt% GO), Pd-Fe/GO (15 wt% Pd - 5 wt% Fe - 80 wt% GO), Pd-Fe/GO (10 wt% Pd - 10 wt% Fe - 80 wt% GO), and Pd-Fe/GO (7 wt% Pd - 13 wt% Fe - 80 wt% GO).

The GO flakes received were cut into a fine powder using razors to create a pellet with evenly mixed particles. The aforementioned powders were then pressed into pellets using a manual press. The nanoparticles were synthesized using LVCC with a pulsed Nd: YAG laser (532 nm). The target was placed in a metal holder adjusted to the focal point of the laser. The top plate was screwed on top of the quartz ring and a vacuum created inside the chamber reduced the pressure to below 9 torr.

Once the pressure was stable, He gas was added to increase the pressure to 300 torr. Purging five times with He followed by a vacuum ensured there were no leaks or contaminant gases left inside the chamber. After the final purge, the pressure was increased to 800 torr. Hot water was circulated around the bottom plate and N_2 (*l*) was circulated over the top plate providing convection as the metal vaporized. The bottom plate was warmed to above 50 $^{\circ}$C and the top plate was cooled to below -30 $^{\circ}$C. The average temperature gradient created was between 60 - 90 $^{\circ}$C.

Before LVCC, the laser was switched from low power to its high energy q-switch mode and operated at 2 watts. As the target was ablated, the laser beam was adjusted around the surface of the target and the pressure was maintained above 800 torr. After ablating as much of the target as possible, paper towels were wrapped around the top plate and kimwipes were placed around the quartz ring to absorb any further condensation.

3. RESULTS AND DISCUSSION

The structures of graphene and graphene oxide can be visualized in Figure 2 where graphene is shown to be a single layer of aromatic carbons and graphene oxide is composed of aromatic carbon atoms as well as reactive oxygen based functional groups. The samples were characterized using Fourier Transform-Infrared (FT-IR) and Ultraviolet-Visible Spectroscopy (UV-Vis). Figure 3 shows the FT-IR spectra of graphene oxide prior to LVCC and the samples after LVCC reduction. The spectrum for GO shows characteristic peaks at 3400 cm^{-1} corresponding to the O-H stretching vibrations, 1720 cm^{-1} corresponding to C=O

stretching vibrations, 1600 cm^{-1} corresponding to C=C stretching vibrations and 1075 cm^{-1} corresponding to C-O stretching. In comparison, the spectra for the samples after LVCC show the complete disappearance of stretching for related oxygen groups indicating the full reduction of graphene oxide.

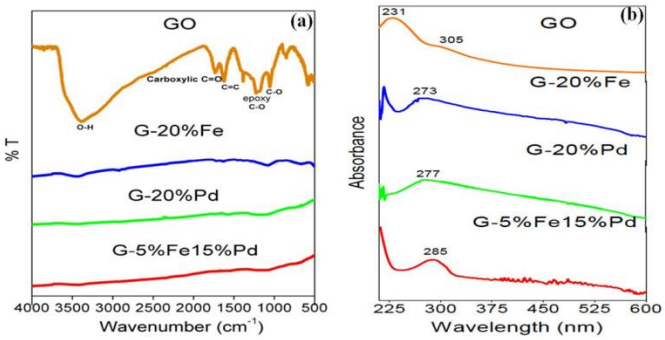

Figure 1. (a) FT-IR spectra of GO and samples after LVCC reduction in He environment, (b) UV-Vis Spectroscopy data of graphene oxide and samples after undergoing LVCC.

The GO spectrum contains a maximum at 231 nm corresponding to $\pi \rightarrow \pi^*$ transitions of aromatic C–C bonds, and a shoulder at 305 nm, which is attributed to $n \rightarrow \pi^*$ transitions of C-O bonds. After LVCC reduction, the UV-Vis spectra shows the maximum peak absorbance is shifted from 231 nm to 273 nm for 20% Fe/ 80% G, 277 nm for 20% Pd/ 80% G and 285 nm for 5% Fe- 15% Pd/ 80% G. The shift to the higher wavelength indicating a lower energy absorbance is due to the removal of the oxygen groups from graphene oxide during LVCC.

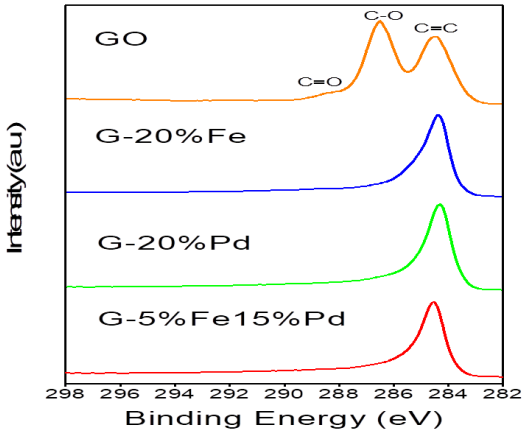

Figure 2. XPS spectra of C1 binding energies for GO and sample after LVCC reduction.

X-ray Photoelectron Spectroscopy (XPS) spectra in Figure 4 compares the C 1s binding energies for GO and LVCC reduced samples. The GO spectrum shows peaks at 285 eV, 286.7 eV and 287.7 eV corresponding to the C=C, C-O and C=O groups, respectively. After laser irradiation, C-O and C=O peaks are removed signifying the reduction of GO.

Figure 5 contains XPS spectra of the Pd3d binding energies for 20% Pd - 80% G and 15% Pd- 5% Fe/ 80% G. The spectra indicate the presence of Pd^0 after reduction due to the binding energies observed at 341 eV (Pd^0 $3d^{3/2}$) and 336 eV (Pd^0 $3d^{5/2}$) which is consistent with those found in literature.

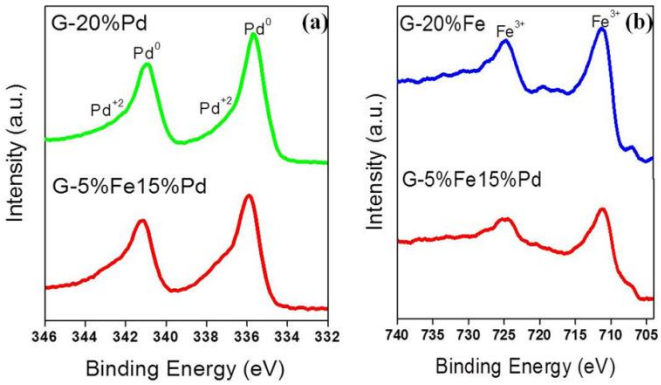

Figure 3. (a) XPS spectra of Pd3d, (b) XPS spectra of Fe2p Binding Energies.

Figures 5 a, b summarizes the XPS data of Fe2p for 20% Fe - 80% G and 15% Pd- 5% Fe - 80% G. The spectra confirms the presence of Fe^{+3} due to the binding energies at 724 eV (Fe^{+3} $2p^{1/2}$) and 711.5 eV (Fe^{+3} $2p^{3/2}$) which is consistent with those found in literature.

The presence and strength of magnetic properties in Fe-G and Pd-Fe/G can be visualized in Figure 6. Once a magnetic field is applied to the samples, a magnetic moment can be observed due to the presence of Fe.

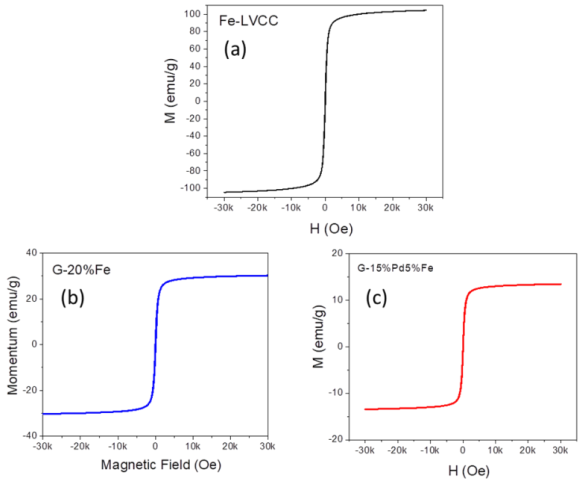

Figure 4. Magnetic data for (a) Fe, (b) Fe/G and (c) Pd-Fe/G**.**

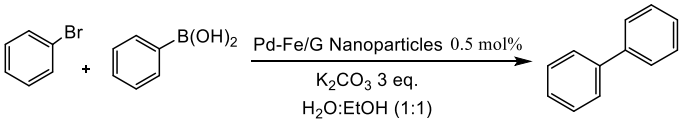

Scheme 1 Suzuki cross coupling reactions using Pd-Fe_3O_4/G

Table 1 depicts the percent conversion obtained after each catalyst was tested in the Suzuki cross-coupling reaction for two runs. The catalyst was subjected to reaction conditions at 80 ^oC using MWI for five minutes.

Table 1. Data collected for recycling of LVCC prepared catalysts. The catalysis was run for 5 minutes at 80 $^{\circ}C$ using MWI.

Catalyst	Run 1 (% Conversion)	Run 2 (% Conversion)
20%Fe – 80%GO	No Reaction	No Reaction
20%Pd – 80%GO	100	-
7%Pd – 13%Fe - 80%GO	93	37
10%Pd – 10%Fe - 80%GO	100	68
15%Pd – 5%Fe - 80%GO	100	86

Without the active component, Pd, no reaction occurred while using the Fe/G catalyst. After increasing the Pd composition, recyclability and activity improved. When more Fe was present, conversion decreased as shown by the 7% Pd - 13% Fe - 80% G where conversion rate for the first run was only 93%. The conversion percent improved with equal compositions of Pd and Fe for both runs. The 15% Pd - 5% Fe - 80% G catalyst proved to be the best catalyst for the cross-coupling reaction which achieved 100% conversion for the first run and 86% conversion for the second run—the highest out of all catalysts for both runs. This is actually consistent with TEM images in Figure 8 as that catalyst showed the best dispersion among other catalysts.

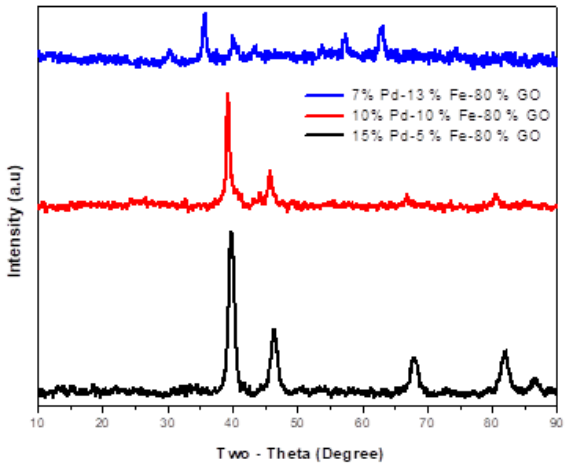

Figure 5. XRD Pattern of selected catalysts prepared by LVCC.

Generally, the XRD pattern shown in Figure 7 clearly indicates that the product is enriched with Fe_3O_4 and metal Pd (0). The palladium shows the typical sharp diffraction peak at 2θ = 40˚. The XRD patterns indicate that the products were all (Fe_3O_4) magnetite with reference code (ICCD-00-003-0863). It is also easily to notice that the sharp diffraction peak at 2θ = 40˚ which is characteristic to palladium and also the characteristic peaks of Fe_3O_4 is shown as a sharp diffraction peak at 2θ = 35˚.

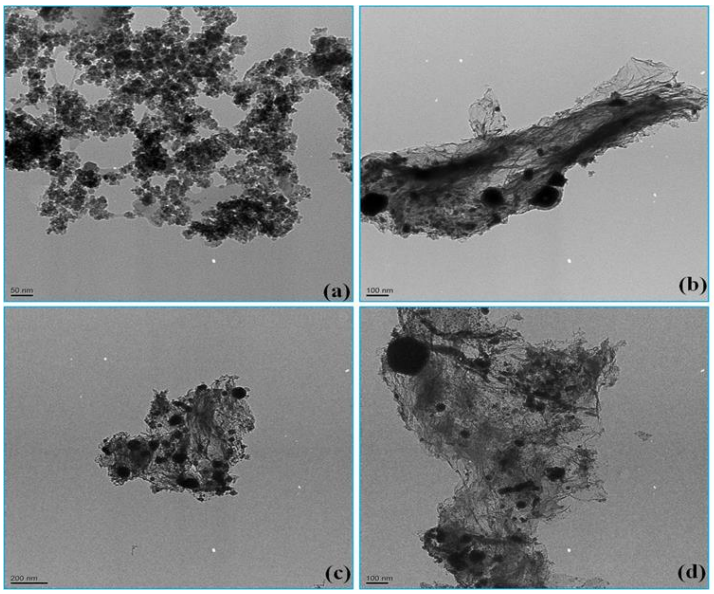

Figure 6. TEM images of (a) 20%Pd – 80%GO, (b) 7%Pd – 13%Fe - 80%GO, (c) 10%Pd – 10%Fe - 80%GO, (d) 15%Pd – 5%Fe - 80%GO.

The very small broad peak around 2θ = 26˚ in Pd- Fe_3O_4/G sample could suggest the presence of a minor component of multilayer graphene. The diffraction peaks (2θ) of Pd- Fe_3O_4/G at 40, 46.8, and 68.2 are ascribed to the (111), (200), and (220) planed of Pd NPs which are similar to pure palladium and also to the peaks of Pd- Fe_3O_4 as shown.

4. CONCLUSIONS

The results indicate that LVCC is superior to other methods that often utilize toxic chemicals for the full reduction of GO. FT-IR data shows the disappearance of GO distinguishing O-H, C=O, C-O, C=C stretching indicating the formation of graphene. UV-Vis data shows peaks red shifted from 230 nm to 280 nm, characteristic of GO reduction and exfoliation. XPS data confirms Pd^{o} and Fe^{+3} present at the surface of the catalyst after reduction. The most effective magnetic catalyst synthesized was the 15% Pd-5% Fe - 80% G. This result can be attributed to the Pd composition being greater than that of the Fe enabling favorable interactions between the Pd and G support increasing catalytic activity and reusability. The least effective catalyst was the 20% Fe - 80% G due to the lack of active component. The effects of manipulating the Pd-Fe/G composition and using different environments in the LVCC process can be investigated further to improve catalysis in cross-coupling reactions.

5. REFERENCES

[1] Compagnini G., et al., Laser assisted green synthesis of free standing reduced graphene oxides at the water-air interface, *Nanotechnology*, 23, 50, **201**2.
[2] Huang L., et al., Pulsed laser assisted reduction of graphene oxide, *Carbon*, 49, 7, 2431-2436, **2011**.
[3] Li Y.B., et al., The catalytic activity of a novel recyclable alkoxypalladium complex in Suzuki reaction, *Tetrahedron*, 68, 40, 8502-8508, **2012**.
[4] Liu Y., et al., Pulsed Laser Assisted Reduction of Graphene Oxide as a Flexible Transparent Conducting Material, *Journal of Nanoscience and Nanotechnology*, 12, 8, 6480-6483, **2012**.
[5] El-Shall M.S., et al., Synthesis and characterization of nanoscale zinc oxide particles: 1. Laser vaporization condensation technique, *Nanostructured Materials*, 6, 1-4, 297-300, **1995**.
[6] El-Shall M.S., et al., Synthesis of nanostructured materials using a laser vaporization-condensation technique, *Nanotechnology: Molecularly Designed Materials*, G.M.G.K.E. Chow, Editor, 79-99, **1996**.
[7] El-Shall, M.S., et al., Synthesis of nanoscale metal-oxide particles using laser vaporization condensation in a diffusion cloud chamber, *Journal of Physical Chemistry*, 98, 12, 3067-3070, **1994**.
[8] Germanenko I.N., et al., Effect of atmospheric oxidation on the electronic and photoluminescence properties of silicon nanocrystals, Pu*re and Applied Chemistry*, 72, 1-2, 245-255, **2000**.
[9] Glaspell G.P., Synthesis of cobalt nitrate hydrate nanoparticles using laser vaporization controlled condensation, *Abstracts of Papers of the American Chemical Society*, 225, U510-U510, **2003**.
[10] Li S.T., M.S. El-Shall, Synthesis of nanoparticles by reactive laser vaporization: silicon nanocrystals in polymers and properties of gallium and tungsten oxides, *Applied Surface Science*, 127, 330-338, **1998**.

[11] Li S.T., Germanenko I.N., El-Shall M.S., Nanoparticles from the vapor phase: Synthesis and characterization of Si, Ge, MoO3, and WO3 nanocrystals, *Journal of Cluster Science*, 10, 4, 533-547, **1999**.
[12] El-Shall M.S., Laser vaporization for the synthesis of nanoparticles and polymers containing metal particulates, *Applied Surface Science*, 106, 347-355, **1996**.
[13] Pithawalla Y.B., Deevi S.C., El-Shall M.S., Preparation of ultrafine and nanocrystalline FeAl powders, *Materials Science and Engineering a-Structural Materials Properties Microstructure and Processing*, 329, 92-98, **200**2.
[14] Li S.T., Silvers S.J., El-Shall M.S., Surface oxidation and luminescence properties of weblike agglomeration of silicon nanocrystals produced by a laser vaporization-controlled condensation technique, *Journal of Physical Chemistry B*, 101,10, 1794-1802, **1997**.
[15] Pithawalla Y.B., El-Shall M.S., Deevi S., Laser based synthesis of intermetallic Cu-Zn nanoparticles and filaments, *Scripta Materialia*, 48, 6, 671-676, **2003**.
[16] Sundar R.S., Deevi S., CO oxidation activity of Cu-CeO2 nano-composite catalysts prepared by laser vaporization and controlled condensation, *Journal of Nanoparticle Research*, 8, 3-4, 497-509, **2006**.
[17] Abdelsayed V., El-Shall M.S., Seto T., Differential mobility analysis of nanoparticles generated by laser vaporization and controlled condensation (LVCC), *Journal of Nanoparticle Research*, 8, 3-4, 361-369, **2006**.
[18] Abdelsayed V., et al., Laser synthesis of bimetallic nanoalloys in the vapor and liquid phases and the magnetic properties of PdM and PtM nanoparticles (M = Fe, Co and Ni), *Faraday Discussions*, 138, 163-180, **2008**.
[19] El-Shall M.S., Abdelsayed V.M., Nanoparticles, filaments, fibers, and tree-like assemblies prepared by laser vaporization controlled condensation, *Abstracts of Papers of the American Chemical Society*, 225, U438-U438, **2003**.
[20] Xi P.X., et al., Surfactant free RGO/Pd nanocomposites as highly active heterogeneous catalysts for the hydrolytic dehydrogenation of ammonia borane for chemical hydrogen storage, *Nanoscale*, 4, 18, 5597-5601, **2012**.
[21] Beckert M., et al., Nitrogenated graphene and carbon nanomaterials by carbonization of polyfurfuryl alcohol in the presence of urea and dicyandiamide, *Green Chemistry*, 17, 2, 1032-1037, **2015**.
[22] Kumar S., et al., Graphene, carbon nanotubes, zinc oxide and gold as elite nanomaterials for fabrication of biosensors for healthcare, *Biosensors & Bioelectronics*, 70, 498-503, **2015**.
[23] Neri G., et al., Engineering of carbon based nanomaterials by ring-opening reactions of a reactive azlactone graphene platform, C*hemical Communications*, 51, 23, 4846-4849, **2015**.
[24] Elazab H., et al., Microwave-assisted synthesis of Pd nanoparticles supported on FeO, CoO, and Ni(OH) nanoplates and catalysis application for CO oxidation, *Journal of Nanoparticle Research*, 16, 7, 1-11, **2014**.
[25] Elazab H., et al., The Effect of Graphene on Catalytic Performance of Palladium Nanoparticles Decorated with FeO, CoO, and Ni (OH): Potential Efficient Catalysts Used for Suzuki Cross-Coupling, *Catalysis Letters*, 147, 6, 1510-1522, 2017.
[26] Elazab H.A., et al., The continuous synthesis of Pd supported on Fe3O4 nanoparticles: A highly effective and magnetic catalyst for CO oxidation, *Green Processing and Synthesis*, 6, 4, . 413-424, 2017.
[27] Elazab H.A., Sadek M.A., El-Idreesy T.T., Microwave-assisted synthesis of palladium nanoparticles supported on copper oxide in aqueous medium as an efficient catalyst for Suzuki cross-coupling reaction, A*dsorption Science & Technology*, 0, 0, 0263617418771777, 2018
[28] Elazab H.A., et al., Highly efficient and magnetically recyclable graphene-supported Pd/Fe3O4 nanoparticle catalysts for Suzuki and Heck cross-coupling reactions, *Applied Catalysis A: General*, 491, 58-69, **2015**.
[29] Mankarious R.A., et al., Bulletproof vests/shields prepared from composite material based on strong polyamide fibers and epoxy resin, *Journal of Engineering and Applied Sciences*, 12, 10, 2697-2701, 2017.
[30] Mohsen W., Sadek M.A., Elazab H.A., Green synthesis of copper oxide nanoparticles in aqueous medium as a potential efficient catalyst for catalysis applications, I*nternational Journal of Applied Engineering Research*, 12, 24, 14927-14930, 2017.
[31] Mostafa A.R., Omar H.A.S., Hany A.E., Preparation of Hydrogel Based on Acryl Amide and Investigation of Different Factors Affecting Rate and Amount of Absorbed Water, *Agricultural Sciences*, 8, 2, 11, 2017.
[32] Radwan M.A., et al., Mechanical characteristics for different composite materials based on commercial epoxy resins and different fillers, *Journal of Engineering and Applied Sciences*, 12, 5, 1179-1185, 2017.
[33] Moussa S., Abdelsayed V., El-Shall M.S., Laser synthesis of Pt, Pd, CoO and Pd-CoO nanoparticle catalysts supported on graphene, *Chemical Physics Letters*, 510, 4-6, 179-184, **2011**.
[34] Moussa S., et al., Pd-Partially Reduced Graphene Oxide Catalysts (Pd/PRGO): Laser Synthesis of Pd Nanoparticles Supported on PRGO Nanosheets for Carbon-Carbon Cross Coupling Reactions, *Acs Catalysis*, 2, 1, 145-154, **2012**.
[35] Moussa S.O., El-Shall M.S., Fabrication of nanostructured nickel and titanium aluminides starting from elemental nanopowders, *Materials Chemistry and Physics*, 112, 3, 1015-1020, **2008**.
[36] Abdelsayed V., Aljarash A., El-Shall M.S., INOR 58-Microwave synthesis of passivated nanoalloys with controlled size and shape, *Abstracts of Papers of the American Chemical Society*, 236, **2008**.
[37] Abdelsayed V., et al., Microwave Synthesis of Bimetallic Nanoalloys and CO Oxidation on Ceria-Supported Nanoalloys, *Chemistry of Materials*, 21, 13, 2825-2834, **2009**.
[38] Abdelsayed, V., et al., Photothermal Deoxygenation of Graphite Oxide with Laser Excitation in Solution and Graphene-Aided Increase in Water Temperature, *Journal of Physical Chemistry Letters*, 1, 19, 2804-2809, **2010**.
[39] AbouZeid, K.M., et al., Shape controlled anisotropic gold nanocrystals via microwave synthesis, *Abstracts of Papers of the American Chemical Society*, 238, **2009**.
[40] AbouZeid K.M., Mohamed M.B., El-Shall M.S., Hybrid Au-CdSe and Ag-CdSe Nanoflowers and Core-Shell Nanocrystals via One-Pot Heterogeneous Nucleation and Growth, *Small*, 7, 23, 3299-3307, **2011**.

6. ACKNOWLEDGEMENTS

The author is grateful for the support from E.A.F, N.S.F, BUE, and VCU for supporting this research. I also acknowledge Jordan Carroll for her kind support as this scientific research is a kind of enhancement for her scientific research including investigating the potential applications in catalysis field. I also express my deep gratitude to Prof. Sherif Moussa and to all members of Prof. El-Shall Research Group and Prof. Gupton Research Group.